Annals Geol. Surv. Egypt. XL (2024). pp. 136- 147
Manuscript ID: ASGE-2312-1006

Integrated Geophysical Studies for Mineral Exploration at Wadi El-Homer, Wadi Ranga Area, South Eastern Desert, Egypt.

BY

Al-Brol, I. [2], Abdelaziz L. Abdeldayem[1], Kamh, S.Z.[1] and Mebad, M. [2]

1. Geology Department, Faculty of Science, Tanta University, Egypt
2. Egyptian General Mineral Resources Authority (EMRA), Abbasiya, Cairo, Egypt

ABSTRACT

The occurrences of mineral ore deposits and disseminated sulfides in Wadi El-Homer are geologically thought to be associated with parts of the shearing fault and the alteration shear zone, which is composed of porphyritic rhyolites - dacite and metamorphosed volcanics highly fractured rocks occupying the all parts of the studied area. Mineralogical analyses that were done on bedrock samples of the oxidized and alteration zones indicated that there are several anomalous spots of minerals reached up to 2.1, 26.1, 9680, 97.5 and 2442 ppm associated with Au, Ag, Cu, Pb and Zn respectively. Therefore, the magnetic, resistivity and induced polarization surveys were applied critically interpreted at Wadi El-Homer area to delineate the mineral ore deposits in terms of depths and extensions. The interpretation of magnetic data was carried out by using the horizontal gradient, source edge detection and source parameter image techniques. The results indicated that the depths of such highly magnetized ore deposits are range from near surface up to 30 m deep. The gradient resistivity survey was carried out simultaneously with IP measurements. The quantitative interpretation technique determined the conductive bodies parameters using the Schulz method (1985) where the depth to the top of the ore body ranged from 17.9 to 70.7 m and the maximum width ranged from 67 to 181 m. The induced polarization (IP) - chargeability data were measured in the time domain. The positive anomalies on the IP-chargeability map are clearly coinciding with the sites of alterations, shears and contact zones. One 2D resistivity/IP imaging profile that was measured along the site of anomalies selected from the magnetic, resistivity and chargeability maps in the study area and inverted using the RES2DINV program. The results of 2D-resistivity and IP inversions indicated that there are anomalous zones of high conductivity and chargeability; indicating probable locations of ore deposits and/or disseminated minerals. On the base of the integrated results, we suggested locations are recommended for drilling to confirm such results and mineral potential of the study area.

Keywords: Mineral exploration, Wadi El-Homer, Ground magnetic, Resistivity, Chargeability methods and 2-D electrical resistivity imaging.

INTRODUCTION

The area of study is located at Wadi El-Homer of South Eastern desert between latitudes 24° 19\` 35" and 24° 20\` 10" N, longitudes 35° 11\` 05" and 35° 11\` 40" E and covering an area about 500 × 500 square meters (Fig. 1-a).

The area of study is discussed by a lot of authors such as [1, 2, 3, 4, 5, 7, 8, 9, 12 and 16] they were considered with the conditions suitable for the occurrence of mineral deposits for mining and its associated minerals.

Detailed surface geophysical surveys including magnetic and electrical methods were conducted on the identified mineralized zones. Surface and subsurface findings will then be integrated to try to detect the lateral and vertical extensions of targeted economic zones.

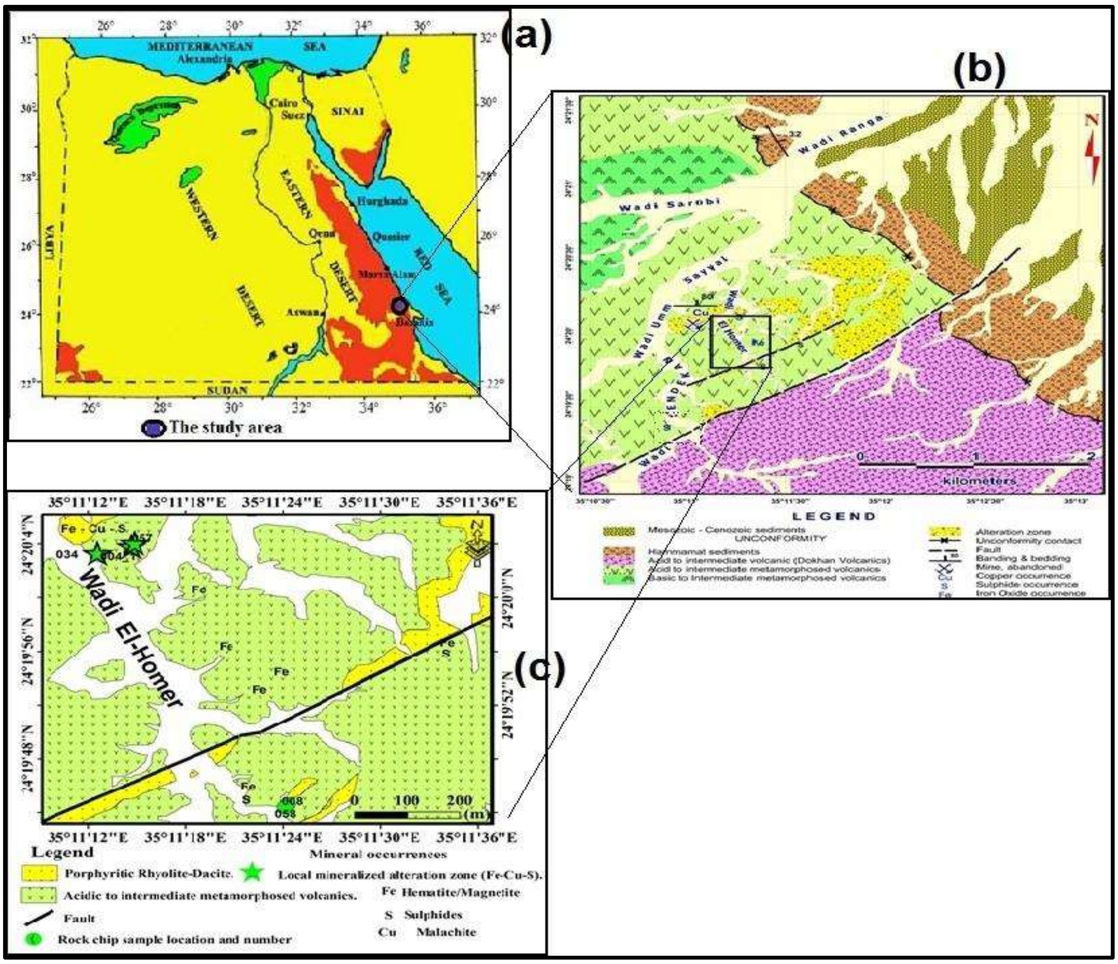

Fig. 1: a) Location map b) regional geological and c) detailed geological maps [4].

GEOLOGIC SETTING

Wadi Ranga represents a part of the northwestern extension of the Arabian-Nubian Shield. The basement rocks of this area are essentially a Pan – African assemblage of a calc-alkaline volcanic group, mafic intrusions (Gabbro), syn- to late- tectonic granites, Dokhan volcnics, Hammamat sediments and dykes [11].

The geology and mineralogy were studied by the Egyptian General Mineral Resources Authority [4]; geologic map and locations of rock samples in Wadi El-Homer area are shown in Fig. (1-b, c). The main rock units which distinguished belong to calc-alkaline metavolcanics. The calc-alkaline metavolcanic rocks are believed to be the oldest rocks exposed in area. They are formed of successive cycles of volcanic flows and sub-volcanic rocks intercalated with bedded volcaniclastic sediments. The study area encloses some mines that have been recently worked. The main mineral occurrences and deposits consist of ilmenite, volcanogenic base metal sulfides (Cu, Pb and Zn) and gold, as well as some talc and ornamental stones of granitic nature. Sulphur, lead, zinc, galena and gypsum mineralization are associated with the middle Miocene sediments, [4].

Along the geological traverses in the El-Homer area, minor quartz veins and zones of alteration and gossans were delineated. Old workings as pits, trench and slags were also found. They are described in detail as follows [4]:

(i) Quartz veins

A few amounts of quartz veins and veinlets were recorded along NE-SW direction, cutting through alteration zones ranging from 10 cm to 1 m in width and varying in color from milky to smoky quartz. The smoky type contains some sulphides and Fe-oxides [4].

(ii) Alteration zones

The outcropping terrains of wadi El-Homer area are locally associated with alteration zones characterized by changes in the mineralogy. The alteration zones are locally characterized by ferruginous zone (hematite and limonite), sulphides minerals (mainly arzenopyrite and few pyrites), calcite, patches of malachite, cubic goethite and some cavities filled by epidote (Fig. 2). The individual alteration zone ranges in thickness from 0.5 m to 10 m and variably extends along E-W direction [4].

Structurally, two principal zones of faults/shears were recorded; the first is NW- SE (parallel to the Red Sea and Gulf of Suez directions) and the second zone is NE-SW (Syrian arc trend) [10].

The results of mineralogical analysis that selected samples from alteration zones and oxidized indicated that there are reached up to 2.1, 26.1, 9680, 97.5 and 2,442 ppm associated with Au, Ag,Cu, Pb and Zn.

Fig. 2: An example of an alteration zone at wadi El-Homer area.

METHODOLOGY

1-MAGNETIC METHOD

550 magnetic stations covering area using two instruments of proton magnetometer made by Scintrex Company (Canada) with accuracy ±1 gamma (nT). Base station instruments were used for recording the daily measurements every 1 minute and to calculate the diurnal variation correction. Field instrument was used for field measurements along eleven lines (Fig. 3); the spacing between the stations along every line varied, ranging from 5 to 10 m in areas of high gradient magnetic anomalies. The corrected magnetic data were gridded and contoured using geosoft program [6] to represent the total magnetic map (Fig.4-a).

Map (Fig.4-a) can be revealed into three zones according to magnetic characters: The highest magnetic anomaly is present in northeastern and northwestern parts with a NNE-SSW trend. The lowest magnetic anomaly occupies the southern and middle parts with NE-SW and NW-SE trends. The medium magnetic anomaly is located in southwestern part of map with NE-SW trend. Clear investigation of the map revealed that the magnetic field increases up with maximum relief of about 41120 nT in northeastern and northwestern parts and decreases to minimum of about 41080 nT in southern and middle parts part of the map. Magnetic trends are almost NNE-SSW, E-W and NE-SW. The highest magnetic anomalies at north eastern and north western parts is separated from medium to low magnetic anomalies in northwestern and southern parts by steep gradient indicating a structural control by a major fault trending in NE-SW and NW-SE directions.

A qualitative relationship can be observed between known geology and magnetic data. The highest anomalies observed on the total magnetic field map seem to correlate with the locations of porphyritic rhyolite-dacite rocks, the medium and low magnetic anomalies correlate with the acidic to intermediate metamorphosed volcanic rocks on the geologic map shown in Fig. 1-c.

A) Horizontal Gradient

Map (Fig.4-b) shows high anomalies that appear in red color representing the contacts and boundaries location and take NE-SW and NW-SE directions.

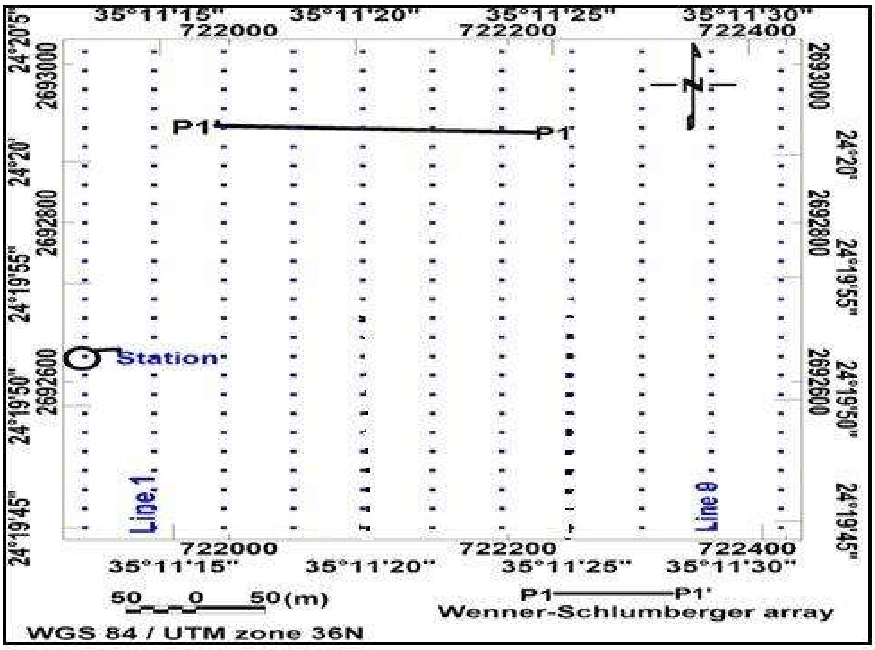

Fig. 3: Geophysical Measurements Locations.

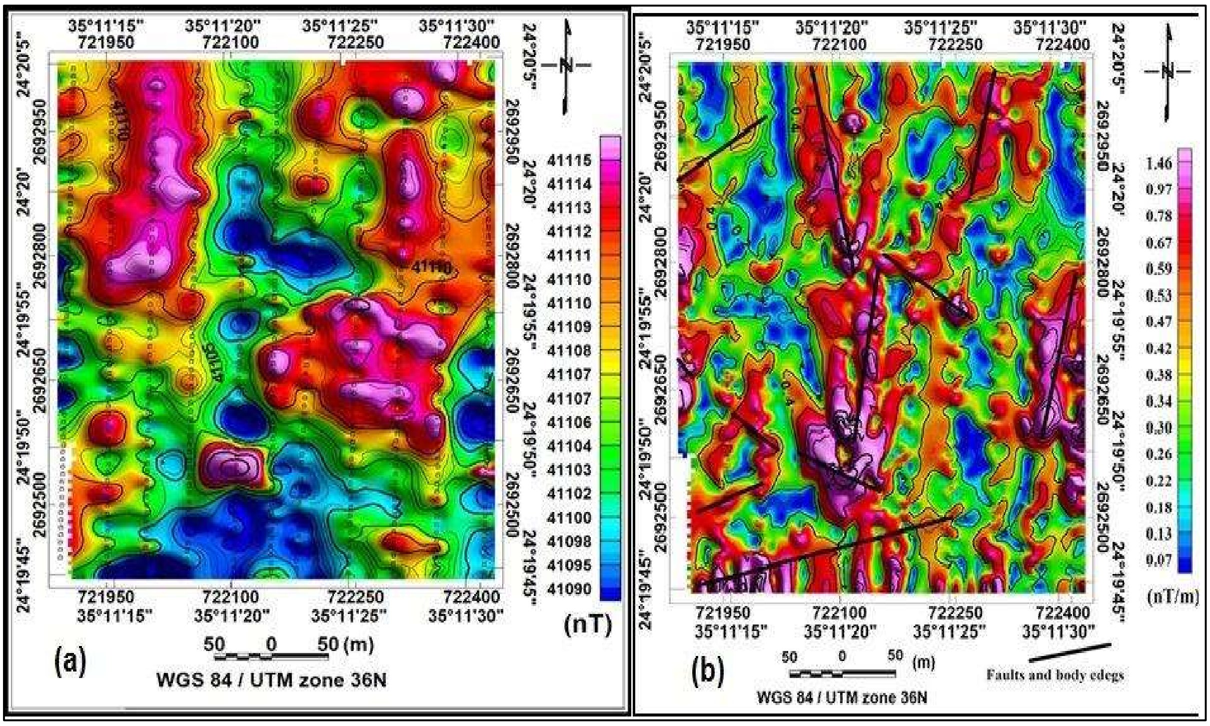

Fig. 4: a) Total magnetic map, b) Horizontal Gradient map.

B) Source Edge Detection (SED)

The edges and geologic boundaries produced from horizontal gradient with rose diagram (Fig. 5) Show major trends along NW-SE, NE-SW directions and minor trends toward E-W and N-S.

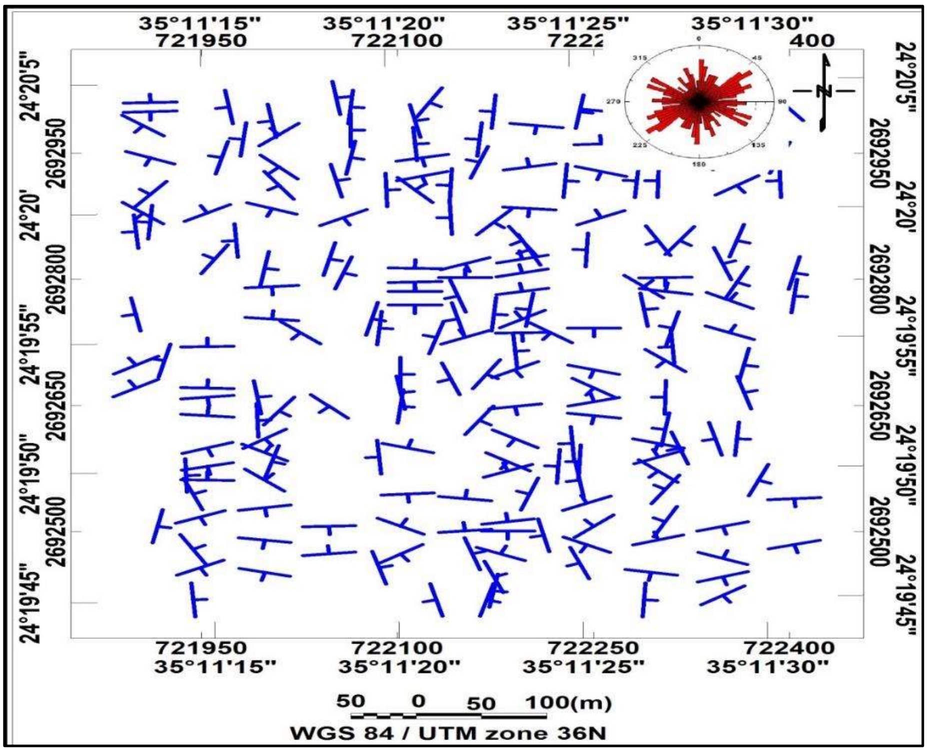

Fig. 5: Source edge detection map produced from horizontal gradient in 4 directions with Rose diagram showing the geological boundaries.

C) **Magnetic Depth Calculation**

- **Source Parameter Imaging (SPI) Technique**

Figure (6) shows shallow and deep magnetic depths of SPI which range from 4 m to 28 m, where shallower depths are located in eastern part and some other places with NE-SW, whereas the deepest are shown in the many parts with NE-SW and NW-SE directions. There is a contact in the eastern part of map as it appears in geologic map shown in Fig. 1-c.

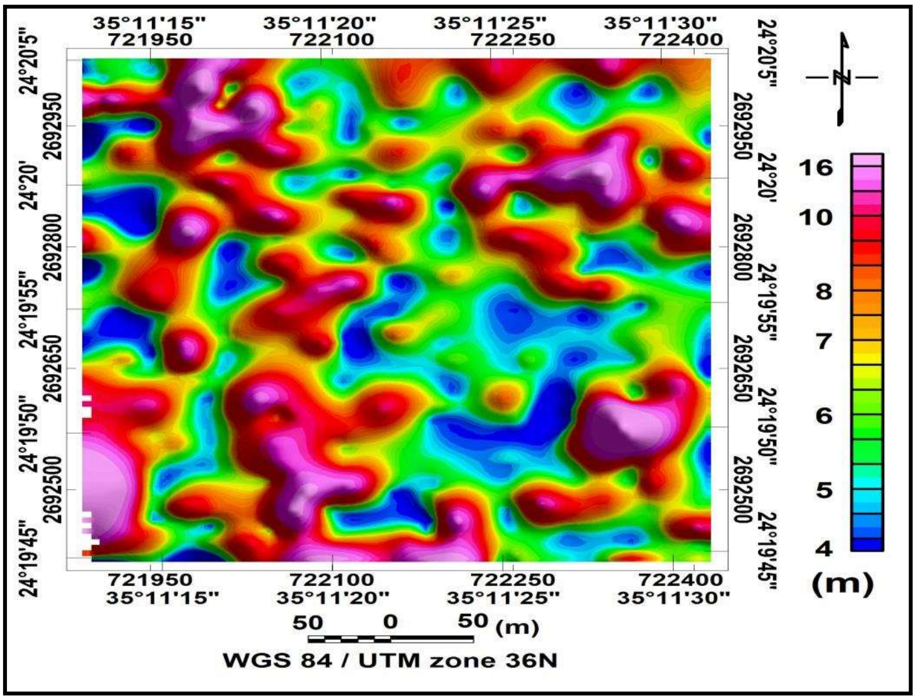

Fig. 6): Source parameter imaging (SPI) with shallow and deep depths.

2-GEOELECTIC DATA

A) Gradient resistivity and (IP)

These surveys were applied also on the grid (Fig.3) pattern in the area to measure the electrical resistivity and chargeability sequentially. The survey has two potential electrodes moved on the stations along lines with spacing (D) or (MN) of 25 meters and two current electrodes fixed in the infinity with interval space (AB) is 1500 meter parallel to these lines.

We used IRIS Resistivity meter, Model ELREC-T to measure the apparent resistivity in Ohm-meters directly for collection resistivity and induced polarization data. Apparent resistivity is measured in Ohm.m and the chargeability interval decay curve in milliseconds. The gradient data obtained are plotted and contoured by Oasis Montaj Program, version standard edition [6].

- **Qualitative Interpretation of Resistivity Data**

Figure 7 showed a distinct large resistivity anomaly zone of low reliefs with magnitude less than 100 Ohm.m. This zone has several widths in northern and southeastern parts. Such anomalies run along the NNW- SSE and E-W directions across the map with greatest width about 250 m occupying the extreme southeastern part while the least width is about 100 m and is found in many parts of the area. A middle zone characterized by relatively high frequency anomalies of elongated small width is founded at western parts. Low resistivity anomaly zones may be alteration or shear zone so it may expect mineral deposits controlled by structure and hydrothermal solutions paths.

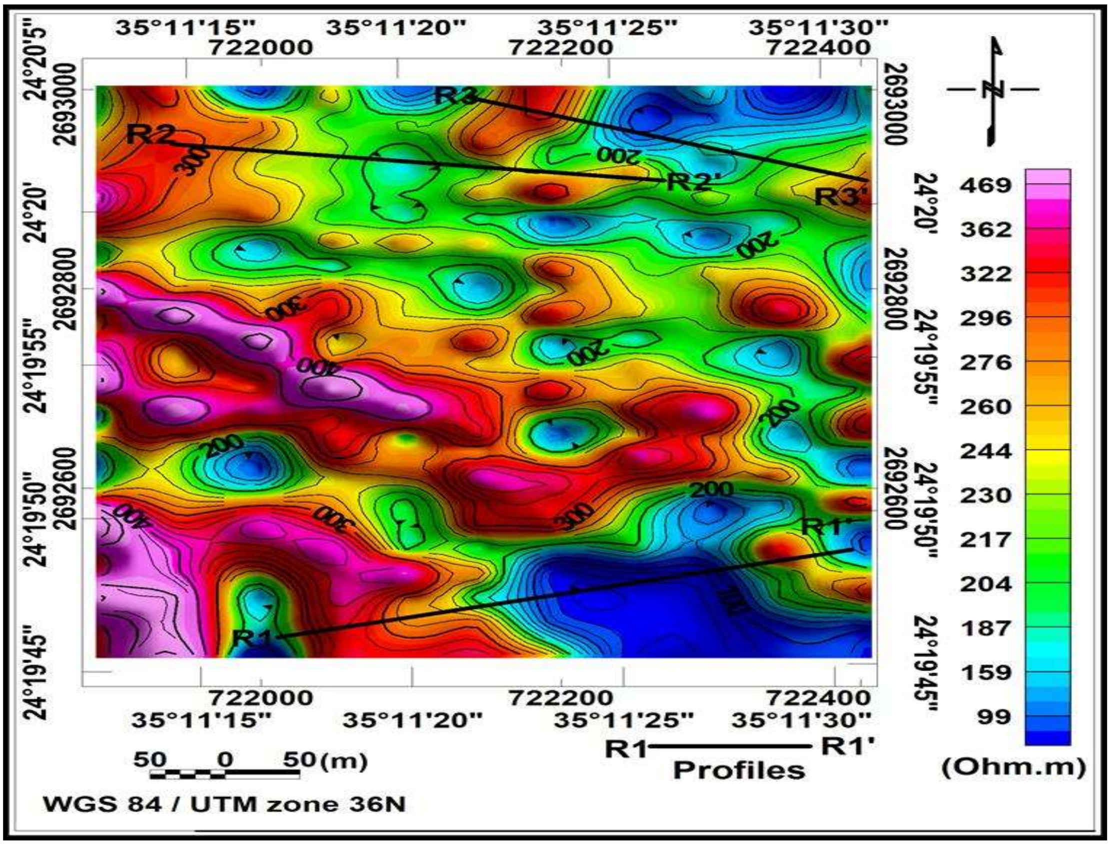

Fig. 7: Gradient Resistivity Map.

- **Quantitative Interpretation of Resistivity**

This interpretation has been carried out through results obtained from three profiles (Fig. 7) and using Schulz method [15].

The parameters were estimated: depth to center of body (Zk), radius (R), depth to top (t) and maximum width (b) using the equations represented in table (1).

Table: (1): Parameters for different body types.

Body type	(Z_k)	(R)	(t)	(b)
Sphere	$0.82\ X^-_M$	$0.75\ \sqrt[3]{\Delta\rho_M} * Z_k$	$(0.82-0.61\ \sqrt[3]{\Delta\rho_M} * X^-_M$	$1.22\sqrt[3]{\Delta\rho_M} * X^-_M$
Cube	$0.82\ X^-_M$	-	$(0.82-0.49\ \sqrt[3]{\Delta\rho_M} * X^-_M$	$1.24\sqrt[3]{\Delta\rho_M} * X^-_M$
Cylinder	$0.58\ X^-_M$	$0.67\ \sqrt[2]{\Delta\rho_M} * Z_k$	$(0.58-0.38\ \sqrt[3]{\Delta\rho_M} * X^-_M$	$0.77\sqrt[3]{\Delta\rho_M} * X^-_M$
Parallelepiped	$0.58\ X^-_M$	-	$(0.58-0.34\ \sqrt[3]{\Delta\rho_M} * X^-_M$	$0.69\sqrt[3]{\Delta\rho_M} * X^-_M$

Where:

$X_M = |X_{M2} - X_{M1}| / 2$ …………….. (Eq. 1)

$\Delta\rho_M = |\rho_M - \rho_{m2}| / \rho_1$ ……………… (Eq. 2)

Table (2) and figure (8) show the results of interpretation. They indicate that (t) ranges from 17.9 to 70.7 meters and (b) reach to 181 meters.

Table: (2): Results of Interpretation Along all Profiles.

Profile no.	body	Z_k (m)	R(m)	t (m)	b (m)
R1	Sphere	109.47	91.2	19	181
	Cube	109.47	-	36.7	145.4
	Cylinder	77.43	60.8	17.9	120.5
	Parallelepiped	77.43	-	24.2	108
R2	Sphere	123	65.6	57.9	130.1
	Cube	123	-	70.7	88.2
	Cylinder	87	34.9	52.8	69.3
	Parallelepiped	87	-	56.4	62.1
R3	Sphere	86.9	61.49	25.9	122
	Cube	86.9	-	37.9	98
	Cylinder	61.48	38.86	24.56	74.8
	Parallelepiped	61.48	-	28.4	67

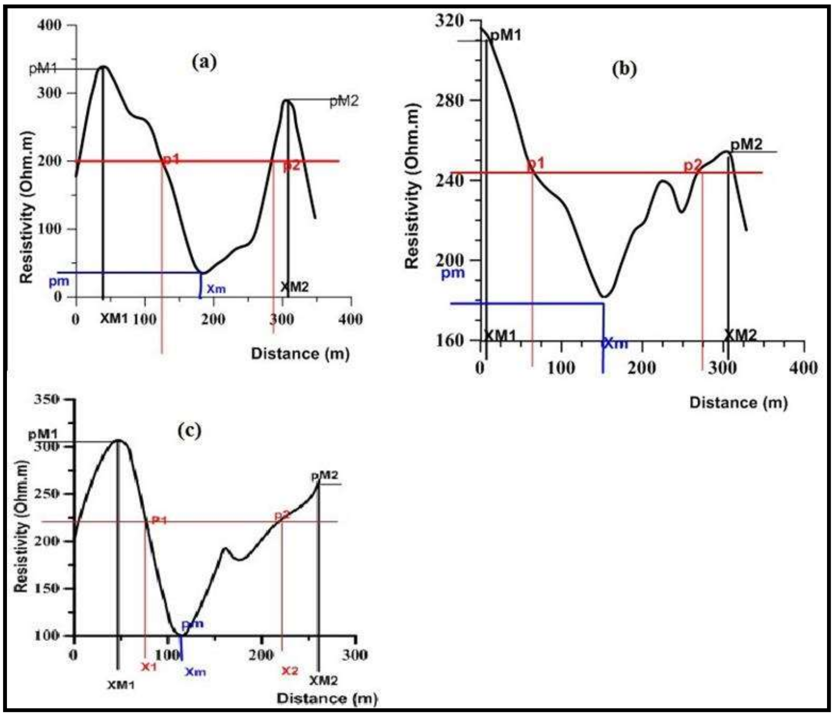

Fig. 8: Interpretation Data along (a) profile R1 (b) profile R2 and (c) profile R3.

- **Gradient chargeability map (IP)**

This map (Fig. 9) is characterized by small amplitudes of chargeability that range from 1 to 39 mSec that seen to characterize most of the study area. The northeastern, western and southeastern parts are characterized by high chargeability values while southwestern and central parts are characterized by low chargeability values. Thereby, the similarity for locating the geoelectric anomalies gives a good observing for presence causative bodies. These bodies showed low resistivity and high chargeability that could reflect mineralized zones. These bodies are selected to cross cut sections oriented across strike. The results suggested refer to the locations of metallic mineralization occurrences and these locations must be followed by detailed geophysical survey in order to in the next stage of field work.

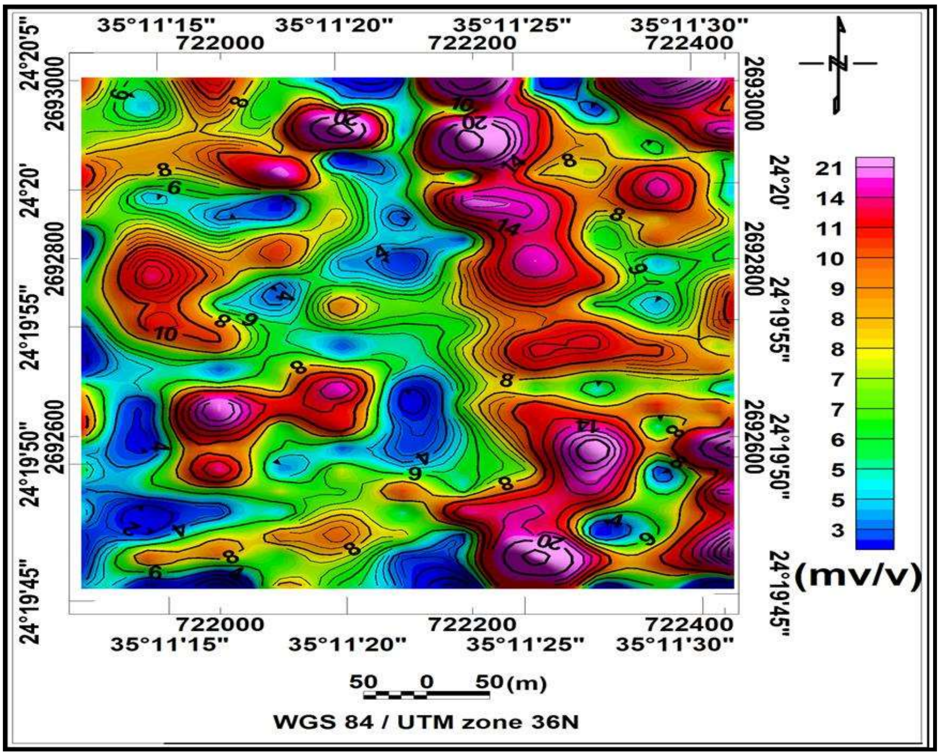

Fig. 9: Gradient IP map

B) RESULTS of 2-D RESISTIVITY/ CHARGEABILITY IMAGING

By comparing the responses from different maps may be a useful monitoring method as well for estimating the promising locations of the conductive mineralization zones, which can be surveyed in the second stage in our explorations by more detailed 2-D resistivity and chargeability imaging techniques. The conductive or nonconductive zones are quantitatively interpreted using suitable interpretation method and consequently the geoelectric cross-sections are constructed over interested anomalies.

Wenner- Schlumberger array is a hybrid between the Wenner and Schlumberger arrays [13] rising out of relatively recent work with electrical imaging surveys. We used three multi-core cables with long 80 meters to collect the data. This configuration is able to give high resolution of the subsurface resistivity distribution.

The imaging techniques were done along one selected profile as detailed stage in area, (Fig. 3). After collecting data in the detailed stage, we did intense filtering before interpretation process to show the best result and locate hidden mineral deposits and determine their extension.

- ***2D Geo-Electrical resistivity/IP imaging along profile (P1-P1')***

Profile (P1-P1') runs across E - W direction (Figs. 3 and 10) with 235 m in length, over anomalous area detected by, resistivity and chargeability surveys (Figs 7 and 9). The interpreted section (P_1-P_1') of resistivity shows disseminated ore minerals of resistivity from 20 to 60 Ohm. meters and high chargeability more than 300 millisecond. It has 80 m width, 35 m thickness and 10 m depth from surface. The change of chargeability value is gradual which refers to sulfide disseminations distributed in the containing rock. There are exposed part of ore (a disseminated sulfide that could be seen by bare eye) at a distance of 100 m approximately from starting point and there are alteration zone on the surface at the end of profile. Results from a rock sample proved to include gold percentage of about 1.2 ppm. This area could be suggested for a test well at a distance of 100 m from section start to a depth of 25 m.

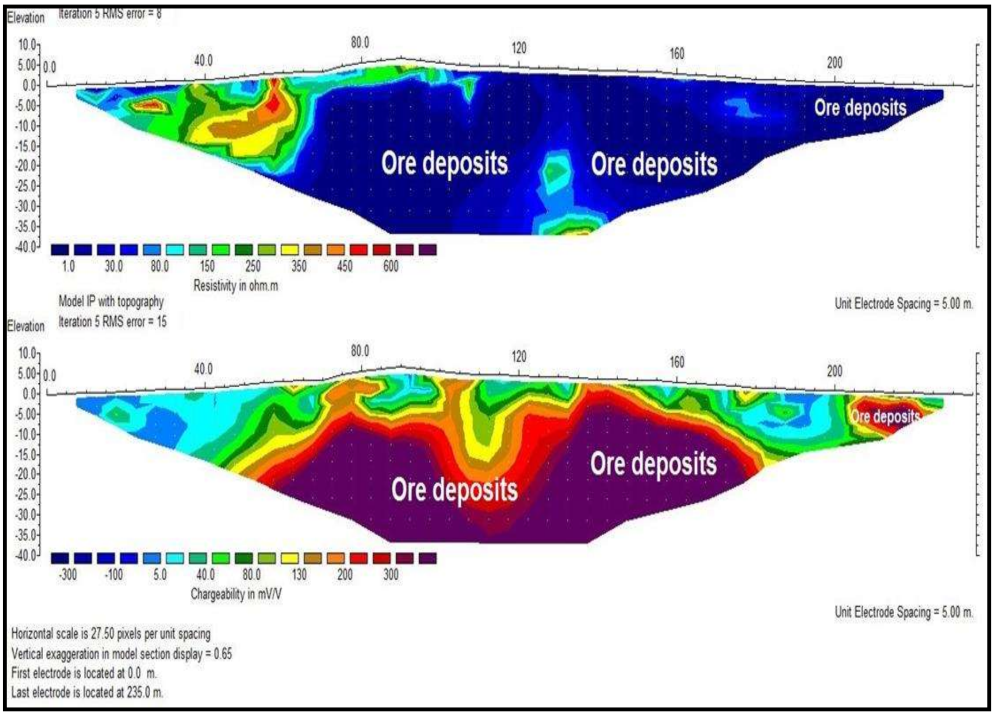

Fig. 10: 2-D model of Geo-Electrical Resistivity/IP Imaging along Profile (P1-P1')

CONCLUSIONS

The geological map showed alteration zones and faults that take NE–SW and NW-SE trends. These faults are clearly detected in the horizontal gradient of the magnetic map. Source parameter imaging "SPI" shows shallow and deep magnetic depths of SPI which range from 4 m to 28 m.

The gradient resistivity and chargeability maps reflect the same trends obtained from low resistivity and high chargeability results in most maps. The depths of the ore body from the gradient resistivity profiles ranges from 8 to 60 m, while maximum width ranges from 28 to 181 meters.

Results of the geological and geophysical surveys indicate the possibility of presence disseminated metallic mineralization and concentrated metallic mineralization at adepth of about 45 m. This result confirms and validate the recorded metallic mineralization (such as ferric oxides, gossans, alteration zones. etc.) identified by integration result.

Based on the integrated results, it is recommended that geophysical surveys must be combined with detailed geological and geochemistry studies, and remote sensing studies and the results should be checked by drilling test.

REFERENCES

Abu El-Rus, M.A., (1991): Geological studies on Abu Ghalaga area, Eastern Desert, Egypt. M.Sc. Thesis, Assiut University, 255p.

Akaad, M.K., Shazly, A.G., Ashmawy, M.H., Abdel Wahed, M.A., (1996): Pan-African basement of Wadi Abu Ghusun-Wadi Khashir district, South Eastern Desert, Egypt. Third International Conference on the Geology of the Arab World, p. 1-16.

Egyptian Geological Survey and Mining Authority (EGSMA), (1997): Geologic map of Jabal Hamata quadrangle, Egypt, scale 1:250000.

Egyptian Geological Survey and Mining Authority (EMRA), (2014): Geological maps of South Wadi Dendekan, Southwest Wadi Ranga, Hamata district, South Eastern Desert, Egypt, internal report, Geological Survey of Egypt.

Fasafous, B.R.B., Attawiya, M. Y., El- Rahmani M.M., (1988): Contribution to the Geochemistry of Volcanics and Associated Mineralization in Hamata Talc Mine, Eastern Desert, Egypt. J. Afr. Earth Sc., oxford, England, V. 7, no. 1. p. 195-199.

Geosoft Program (Oasis Montaj, ver.6.4, 2), (2007): Geosoft Mapping and Application System, Inc, Suite 500, Richmond St. West Toronto, ON Canada N5SIV6.

Girgis M.H. (1969): Mineralogical Studies on Some Titaniferous Iron Ores, South Eastern Desert, Egypt. M.Sc., Cairo Univ., Egypt.

Girgis M.H. (1975): Mineralogical, Petrological and Geochemical Studies on Some Titaniferous Iron Ores of Eastern Desert, Egypt. Ph.D., Cairo Univ., Egypt.

Kamel, E.K., (1969): Geology of The Area around Hamata Talc Mine, Eastern Desert. Ph.D. Thesis, Assiut University.

Kroner, A., Greiling, R., Reisch mann, T., Hussein, I.M., Stern, R.J., Kruger, J., and Zimmer, M, (1987): Pan-African Crustal Evolution in the Nubian Segment of northeast Africa. Ann. Geophy. Union, Spec. Publ. 17.

Mostafa, H. A. Mohamed, A. F. Abd El-Moula, S. A. Attia and M. A. Moussa (1996): Geology of Tarafawi-Abu Ghusun area, South Eastern Desert, Egypt. Final Report of Expedition 7/93. Internal Report, Geol. Surv. Egypt, No. 2/96.

Nessim S.; Afia M.S.; Fahim M. and Foda A.A; (1954): Report on The Prospecting Work Carried out in Wadi Hamata Area, South Eastern Desert. Department of Mines and Quarries, Mineral Research Section, Cairo.

Pazdirek, O. and Blaha, V., (1996): Examples of Resistivity Imaging Using ME-100 Resistivity Field Acquisition System. EAGE 58th Conference and Technical Exhibition Extended Abstracts, Amsterdam.

RES2DINV ver. 3.4 (2003): Rapid 2D resistivity & IP inversion using the least-squares method Geoelectric Imaging 2D & 3D, Geotomo Software, Malaysia

Schulz R. (1985): Interpretation and depth investigation of gradient measurements in direct current geoelectrics Geophys. Prosp., 33, 40–53

Shukri, N.M., Mansour, M.S., (1980): Lithostratigraphy of Um Samiuki District, Eastern Desert. Egypt. Inst. Appl. Geol. Jeddah Bull., No.4, v. 3, p. 127-134.